NRC Research Press

ARTICLE

Stabilizing, non-covalent interactions in the solid state structure of novel aryltin hydrides and halogenides

Cathrin Zeppek, Roland C. Fischer, Ana Torvisco, and Frank Uhlig

Abstract: A group of novel aryltin chlorides, bromides and hydrides (Ar_nSnY_{4-n}) (Ar = *o*-tolyl, 2,6-xylyl, 1-naphthyl, 2-naphthyl, *p*-*n*-butylphenyl; Y = Cl, Br, H) have been synthesized and structurally characterized via X-ray diffraction. These compounds display noncovalent intermolecular interactions in the form of edge to face, π–π stacking and C–H···π interactions resulting in discrete arrangements in the solid state. The strength of these interactions and their effect on resulting structural parameters, as well as the consequence of the aromatic substituent on the type of interactions present, will be highlighted and discussed.

Key words: aryltin halides, aryltin hydrides, crystal packing motifs, intermolecular interactions, π–π stacking.

Résumé : De nouveaux chlorures, bromures et hydrures d'arylétain (Ar_nSnY_{4-n}) (où Ar = *o*-tolyl, 2,6-xylyl, 1-naphthyl, 2-naphthyl ou *p*-*n*-butylphenyl, et Y = Cl, Br ou H) ont été synthétisés et leur structure été déterminée par cristallographie aux rayons X. Ces composées présentent des interactions intermoléculaires non covalentes de type bord-face, empilement π et C–H···π, qui conduisent à des arrangements distincts à l'état solide. La force de ces interactions, leur effet sur les caractéristiques structurelles qui en résultent et l'impact du substituant aromatique sur les types d'interaction présents, seront exposés et étudiés. [Traduit par la Rédaction]

Mots-clés : halogénure d'arylétain, hydrure d'arylétain, motifs d'un empilement cristallin, interactions intermoléculaires, empilement π.

Introduction

The synthesis and detailed characterization of various tetraaryl stannanes (Ar_4Sn) exhibiting aliphatic substituents on the aromatic ring via a Grignard reaction pathway has been well established.[1–2] These compounds serve as starting materials for the generation of aryltin halogenides (Ar_nSnX_{4-n}), which themselves act as major precursors for the formation of highly oxygen and temperature labile aryltin hydrides (Ar_nSnH_{4-n}). Hence, the majority of reported crystallographically studied aryl substituted tin species have been tetraaryl stannanes[3–9] and aryltin monochlorides[10–19] and dichlorides.[20–27] However, solid state examples of trichlorides are limited, and the only aryltin hydride species to have been characterized crystallographically is Mes_2SnH_2 (Mes = 2,4,6-trimethylphenyl).[28] Very recently, we reported the synthesis, detailed characterization, and DFT studies of novel aryltin chloride and hydride species.[2] Their potential use as starting materials for polyarylstannanes provided the motivation to establish the generation of aryltin trihydrides displaying a hitherto more or less neglected compound class of organotins. On the way towards these crucial starting materials, we were able to generate a large variety of aromatic tin compounds as well as elucidating their solid state structure via single crystal X-ray crystallography. While not previously mentioned in literature, tetraaryl stannanes, aryltin chlorides, bromides, and hydrides exhibit noncovalent interactions in the solid state, stemming from the aromatic substituents. The role of aromatic noncovalent interactions in the stabilization of compounds in solid state and their importance in chemical and biological processes have been well documented.[29–33] However, their presence and ultimately their effect on aryltin species have never been studied.

In an effort to expand the existing library of compounds and study the underlying factors leading to solid state structures, we present a series of novel tetraaryl stannanes (**1–3**) and aryltin halogenides (**4–7**) with aryl substituents ranging in steric demand from *o*-tolyl to naphthyl. In addition, a novel aryltin monohydride species 2,6-xylyl$_3$SnH (**8**) is presented. The types of noncovalent interactions present in these systems will be highlighted and compared to previously reported compounds. In addition, the nature of the aromatic substituent and its direct effects on the type of electrostatic interaction that arises in these structures will be discussed.

Results and discussion

Synthesis

For the generation of aryltin halogenides and hydrides (**4–9**), the corresponding tetraaryl stannane (**1–3**) was synthesized first and then used for all further conversions (Scheme 1). In each case, the commercially available arylbromide was converted into the Grignard reagent in THF or Et_2O, respectively, and subsequently treated with $SnCl_4$ to generate the corresponding tetraaryl stannane (Ar_4Sn).[1] The synthesis of tetraaryl stannanes as well as their use as precursors in the generation of aryltin halogenides and hydrides have been well established.[1–2] In the case of the sterically demanding 2,6-xylyl aryl residue, the formation of 2,6-xylyl$_4$Sn was not observed, and 2,6-xylyl$_3$SnBr (**4**) was isolated. This halogen interchange has also been described for the preparation of sterically

Received 31 October 2013. Accepted 26 January 2014.

C. Zeppek, R.C. Fischer, A. Torvisco, and F. Uhlig. TU Graz, 6330 Institut für Anorganische Chemie, 8010 Graz, Stremayrgasse 9/IV, Austria.
Corresponding author: Ana Torvisco (e-mail: ana.torviscogomez@tugraz.at).

This article is part of a Special Issue commemorating the 14th International Conference on the Coordination and Organometallic Chemistry of Germanium, Tin, and Lead (ICCOC-GTL 2013) held in Baddeck, NS, July 2013.

Scheme 1. General synthetic scheme towards tetraaryl stannanes and aryltin derivatives.

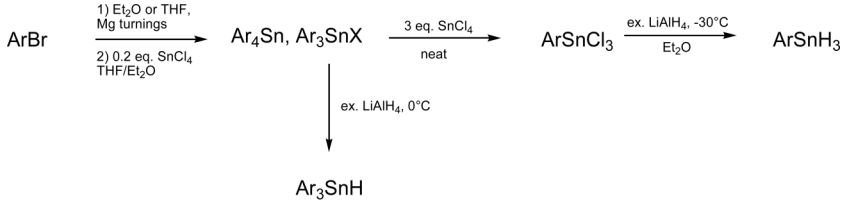

Ar = *o*-tolyl (**5**), 2,6-xylyl (**4**,**8**), 1-naphthyl (**1**), 2-naphthyl (**2**,**6**) *p*-^{n}butylphenyl (**3**,**7**,**9**).

encumbered species of mesityl tin compounds.[34] Isolation of the different aryltin species as well as optimization of the reaction conditions to get a single product were not necessary, because the mixtures were treated with excess $SnCl_4$ to generate the desired aryltin trichlorides (**5–7**), according to the Kozeshkov equilibrium.[35–38]

To obtain the aryltin hydride species (Ar_3SnH **8**, $ArSnH_3$ **9**), the respective aryltin monobromide and trichloride were subjected to a hydrogenation reaction in Et_2O with an excess of $LiAlH_4$ (lithium aluminum hydride) as described in literature.[39] Compounds 2,6-Xylyl$_3$SnH (**8**) and *p*-*n*-butylphenylSnH_3 (**9**) were generated at 0 and –30 °C, respectively, and isolated by gently removing the solvent under reduced pressure. Afterwards, liquid aryltin hydrides were distilled at room temperature (RT) using a turbomolecular pump, and solid hydrides were recrystallized. The thermal instability of organotin hydrides, as well as the affinity towards oxygen, is reported to increase with replacement of each organic group by a hydrogen atom.[40] As a result, *p*-*n*-butylphenylSnH_3 (**9**) is a very unstable liquid, sensitive towards high temperature and oxygen and is stored at –80 °C under inert conditions like other reported tin trihydrides.[2,41]

^{119}Sn NMR Spectroscopy

Table 1 summarizes ^{119}Sn NMR shifts of all included compounds (**1–9**) measured in C_6D_6 as well as published shifts of substituted triaryltin bromides and phenyl$_n$SnY_{4-n} (Y = Cl, Br, H) species for comparison. For the aryltin chloride species (Ar_nSnCl_{4-n}), an increase in number of chlorines results in a lower shielding of the ^{119}Sn nucleus, thus in a high field shift in ^{119}Sn NMR, which has recently been extensively studied.[2] In this manner, the listed shifts fall in an expected range according to the number of halogens or hydrogens bonded to the tin. ^{119}Sn shifts of the presented tetraaryl stannanes lie between –118 to –122 ppm, whereas aryltin chlorides are high field shifted (–58 to –64 ppm). Triaryltin bromides show an increased high field shift in comparison to their corresponding chlorides, as seen for Ph_3SnCl (–45 ppm, $CDCl_3$) and Ph_3SnBr (–60 ppm, $CDCl_3$).[42] In addition, aryl moieties exhibiting methyl substitution in both ortho positions of the aromatic ring bonded to the Sn lead to high field shift increases in comparison to the nonsubstituted phenyl derivative (phenyl$_n$SnY_{4-n}). This effect has been described in detail for the 2,6-xylyl and mesityl residue and is explained by hyperconjugation, which causes the Sn atom to exhibit a slightly higher electron density.[2] The compound 2,6-xylyl$_3$SnBr (**4**) shows the lowest shift for all reported triaryltin bromides.

Crystallographic studies

The presence of aromatic secondary interactions and their importance as stabilizing factors for these aryltin derivatives in the solid state has been rarely discussed or simply overlooked. Specifically, interactions attributed to the aromatic substituents including π–π stacking, edge to face, or C–H···π interactions have been neglected. Figure 1 summarizes the types of aromatic noncovalent interactions and acceptable ranges found in biological and organic systems.[29–31] All novel aryltin compounds presented display noncovalent interactions in the solid state through the aromatic substituents. These stabilizing interactions are described and compared to those present in previously reported species. In addition, interactions for model aromatic systems (benzene, toluene, naphthalene) are included for comparison.

Tetraaryl stannanes (1–3)

Compounds 1-naphthyl$_4$Sn (**1**), 2-naphthyl$_4$Sn (**2**), and *p*-*n*-butylphenyl$_4$Sn (**3**) are comparable to previously reported tetraaryl stannanes (Table 2). Each Sn atom is in a near tetrahedral environment with C-Sn-C angles ranging from 107°–114°. With respect to averaged Sn–C bonds, these fall within a narrow range of 2.13–2.15 Å and are not affected by the degree of bulkiness caused by the organic substituent on Sn. In most cases and as seen for phenyl$_4$Sn,[3] tetraaryl stannanes crystallize in high symmetry space groups, mainly tetragonal, and display highly ordered packing motifs. These consist of columns of symmetry related molecules. This packing motif is also seen in 2-naphthyl$_4$Sn (**2**) (Fig. 2), which crystallizes in the *I*-4 space group. For this compound, each of these columns consists of interlocking neighbouring molecules by edge to face interactions (2.50 Å) through the naphthyl substituents (Table 2). These values fall within range for edge to face interactions found in biological and organic systems (2.4–3.1 Å).[29–30] While not reported in literature, slightly longer interactions on average are observed for phenyl$_4$Sn (2.95 Å). In the case of 1-naphthyl$_4$Sn (**1**), which crystallizes in the monoclinic space group $P2_1/n$, discrete column formation is not observed in agreement with the lower symmetry. This results in the molecules orienting themselves to maximize interactions between neighbouring molecules, and numerous edge to face interactions ranging from 2.53–2.95 Å are observed. 1-Naphthyl$_4$Sn (**1**) and 2-naphthyl$_4$Sn (**2**) compare well with the herringbone packing structure of naphthalene, which also exhibits edge to face interactions (2.81 Å).[43]

Introduction of *n*-butyl groups in the para position of the phenyl substituent in *p*-*n*-butylphenyl$_4$Sn (**3**) results in crystallization in the low symmetry space group *P*-1. This is due to the higher degree of rotation of the *n*-butyl groups, compared to the *t*-butyl groups of *p*-*t*-butylphenyl$_4$Sn,[9] which is tetragonal ($P4_2/n$). In addition to the presence of edge to face interactions (2.96 Å) in compound **3**, C–H···π interactions are observed between the methylene hydrogens of the butyl substituents and the phenyl groups of neighbouring molecules (2.91 Å) (Table 2). However, despite the potential for the *t*-butyl group in *p*-*t*-butylphenyl$_4$Sn for C–H···π interactions, only an edge to face interaction (2.98 Å) is observed between the phenyl substituents of neighbouring molecules.

Aryltin hydrides and bromides (4, 8)

While compounds **1** and **2** show a propensity towards edge to face interactions due to the nature of the naphthyl moiety, addition of methyl groups on the aryl substituent of Sn should lead to C–H···π interactions being preferred in packing motifs. This is indeed the case for 2,6-xylyl$_3$SnBr (**4**) and 2,6-xylyl$_3$SnH (**8**), where the molecules in the solid state arrange themselves to maximize these interactions (Table 3). It should be noted that Aryl$_3$SnCl

Table 1. ^{119}Sn NMR shifts (C_6D_6) of all included compounds.

Compound	^{119}Sn NMR shift (ppm)	Compound	^{119}Sn NMR shift (ppm)
Aryl$_4$Sn		**ArylSnCl$_3$**	
phenyl$_4$Sn[2]	–127	phenylSnCl$_3$[2]	–61
1-naphthyl$_4$Sn (**1**)	–119	*o*-tolylSnCl$_3$ (**5**)	–61
2-naphthyl$_4$Sn (**2**)	–118	2-naphthylSnCl$_3$ (**6**)	–64
p-*n*-butylphenyl$_4$Sn (**3**)	–122	*p*-*n*-butylphenylSnCl$_3$ (**7**)	–58
Aryl$_3$SnBr		**Aryl$_3$SnH**	
phenyl$_3$SnBr[1]	–60[a]	phenyl$_3$SnH[2]	–163
o-tolyl$_3$SnBr[1]	–54[a]	2,6-xylyl$_3$SnH (**8**)	–287
m-tolyl$_3$SnBr[1]	–57[a]	**ArylSnH$_3$**	
p-tolyl$_3$SnBr[42]	–52[a]	phenylSnH$_3$[2]	–345
2,6-xylyl$_3$SnBr (**4**)	–132	*p*-*n*-butylphenylSnH$_3$ (**9**)	–345
mesityl$_3$SnBr[1]	–121[a]		

[a]measured in $CDCl_3$.

Fig. 1. Orientations of aromatic noncovalent interactions and accepted ranges.[29–31]

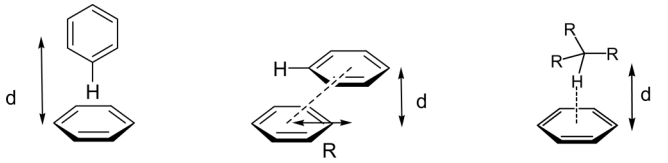

a) Edge to Face
d = 2.4–3.1 Å

b) Parallel Displaced
d = 3.4–3.6 Å
R = 1.6–1.8

c) C–H···π
d = 2.3–3.4 Å

Table 2. List of Sn–C bond lengths and noncovalent interactions for selected tetraaryl stannanes and model aromatic systems.

	Space group	Sn–C (Å) (avg.)	Edge to face (Å)	C–H···π (Å)
phenyl$_4$Sn[3]	*P*-42$_1$*c*	2.139(5)	2.86–3.14	—
o-tolyl$_4$Sn[4]	*P*-42$_1$*c*	2.152(5)	—	3.36
m-tolyl$_4$Sn[5]	*I*4$_1$/*a*	2.150(3)	3.13	—
p-tolyl$_4$Sn[6]	*I*-4	2.147(6)	2.78	3.22
3,5-xylyl$_4$Sn[7]	*P*-42$_1$*c*	2.134(5)	—	3.39
2,4-xylyl$_4$Sn[8]	*P*-1	2.139(2)	3.07	2.95–3.39
p-ethylphenyl$_4$Sn[9]	*C*2/*c*	2.129(4)	3.21	3.24
p-*n*-butylphenyl$_4$Sn (**3**)	*P*-1	2.137(2)	2.96	2.91
p-*t*-butylphenyl$_4$Sn[9]	*P*4$_2$/*n*	2.138(5)	2.98	—
1-naphthyl$_4$Sn (**1**)	*P*2$_1$/*n*	2.154(6)	2.53–2.95	—
2-naphthyl$_4$Sn (**2**)	*I*-4	2.145(7)	2.50–3.15	—
benzene[33]	*Pbca*	—	2.84	—
toluene[33]	*P*2$_1$/*c*	—	2.78	2.61
naphthalene[43]	*P*2$_1$/*a*	—	2.81	—

species are better studied and therefore not included in these discussions.[10–13,15] As shown in Fig. 3, molecules of compound 2,6-xylyl$_3$SnBr (**4**) are arranged in a staggered formation creating chains propagated through C–H···π interactions (2.78 Å) from a methyl group and a neighbouring 2,6-xylyl substituent. These interactions are well within range for reported C–H···π interactions (2.3–3.4 Å).[29] These latter are also visible in the solid state packing motif for toluene,[33] which in addition to edge to face interactions (2.78 Å), exhibits closer C–H···π interactions from the methyl group (2.61 Å) (Table 2). While no Sn–Br interactions were seen between neighbouring molecules, the closest distances being well over 8 Å, C–H···Br interactions were observed (3.03–3.10 Å) between chains. Compared to phenyl$_3$SnBr (2.114(8) Å), a slight increase in the average Sn–C bond lengths is seen for 2,6-xylyl$_3$SnBr (**4**) (2.164(8) Å) and mesityl$_3$SnBr (2.169(5) Å), consistent with increased steric bulk around the Sn center due to the methyl groups at the 2- and 6-positions of the aryl substituent (Table 3). This increased steric bulk around the Sn center is also manifested by an elongated Sn–Br bond in 2,6-xylyl$_3$SnBr (**4**) and mesityl$_3$SnBr (2.547(1) Å), compared to phenyl$_3$SnBr (2.495(2) Å). While 2,6-xylyl$_3$SnBr (**4**) does not exhibit any edge to face interactions within acceptable ranges, the lack of methyl groups in Ph$_3$SnBr allows for very close contacts (2.63–3.14 Å).

Synthetic applications for triorgano tin hydrides (R$_3$SnH) are a well investigated field in organometallic and organic synthesis, especially in mediating radical additions, rearrangement and elimination reactions.[47] Furthermore in the last decade, organotin dihydrides (R$_2$SnH$_2$) have been explored as precursors in the formation of polymeric materials exhibiting a linear backbone of covalently bonded tin atoms.[28,48–49] However, the solid state structures of organotin hydrides have not been well studied. While alkyl tin hydrides are liquid, the only solid state examples of aryltin hydrides known to date have been isolated by our working group and include mesityl$_2$SnH$_2$,[28] phenyl$_3$SnH,[44] and 2,6-xylyl$_3$SnH (**8**) (Table 3). As mentioned above, presence of methyl groups at the 2- and 6-position of the aryl substituent results in a slight increase of the average Sn–C bond length in 2,6-xylyl$_3$SnH (2.159(5) Å) and mesityl$_2$SnH$_2$ (2.154(9) Å), compared to phenyl$_3$SnH (2.141(4) Å). In the case of 2,6-xylyl$_3$SnH, Sn–H was not reliably located in the difference map, which is a common problem with light atoms (hydrogen) located next to heavy atoms because of their poor scattering abilities. For mesityl$_2$SnH$_2$,[28] which is a dihydride, Sn–H bonds are on average 1.669(2) Å. In phenyl$_3$SnH,[44] the hydrogen at the tin atom was located in the difference map exhibiting the first experimental Sn–H bond length for a monostannane (1.13(5) Å).

Nevertheless, packed structures of **8** (Fig. 4) reveal staggered chains of alternating edge to face (2.87 Å) and C–H···π interactions (2.70–2.81 Å). The lack of these methyl substituents on phenyl$_3$SnH results exclusively in the presence of edge to face interactions, however, an additional Sn–H···π interaction, 3.092(3) Å, is observed.[44] In mesityl$_2$SnH$_2$, only C–H···π interactions ranging from 2.70 and 2.75 Å are observed.

Aryltin trichlorides (5, 6)

Until a recent contribution from this working group,[2] only two examples of structurally characterized aryl trichloro stannanes had been reported in literature (Table 4).[50–51] The compounds (2,6-Mes)PhSnCl$_3$ (Mes = (2,4,6-Me)Ph) and Ph*SnCl$_3$ (Ph* = (2,6-Trip)Ph, Trip = (2,4,6-iPr)Ph) employ sterically hindered substituents containing methylated aryl moieties on the phenyl substituents and only exhibit C–H···π interactions (Table 4). More recent examples include methyl-substituted phenyl and naphthyl derivatives. In the case of 1-naphthylSnCl$_3$[2]and 2-naphthylSnCl$_3$ (**6**), large deviations from Sn–C or Sn–Cl bond lengths are not observed. However, the naphthyl derivatives display much different crystal packing motifs than for the aforementioned bulkier substituents. In both 1-naphthylSnCl$_3$ and 2-naphthylSnCl$_3$ (**6**) (Fig. 5), the

Fig. 2. Crystal packing diagram for 2-naphthyl$_4$Sn (**2**). Edge to face interactions are highlighted by dashed bonds. All non-carbon atoms shown as 30% shaded ellipsoids. Hydrogen atoms not involved in intermolecular interactions removed for clarity.

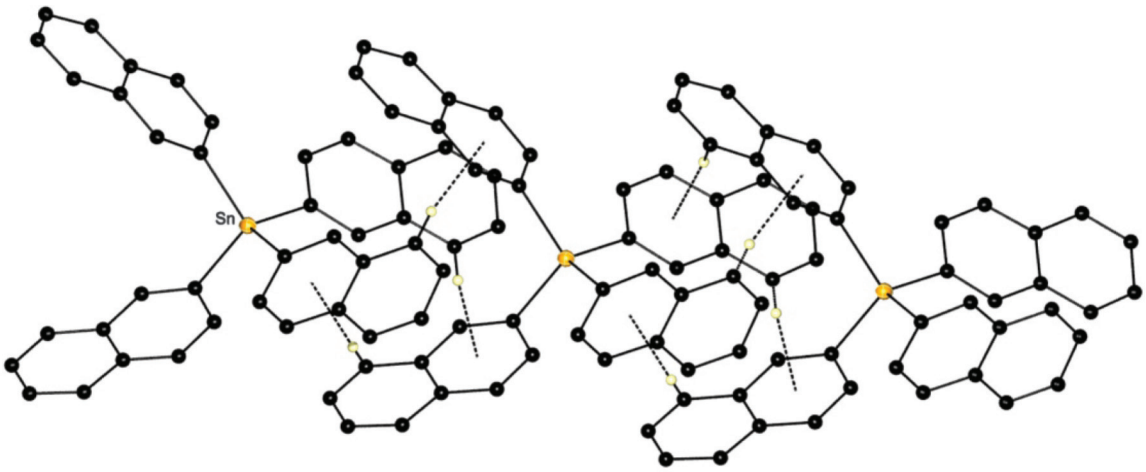

Table 3. List of Sn–C bond lengths and noncovalent interactions for selected aryl tin hydrides and bromides.

	Space group	Sn–C (Å) (avg)	Sn–X (Å) (avg)	Edge to face (Å)	C–H···π (Å)	C–H···Br (Å)	Sn–H···π (Å)
phenyl$_3$SnH[44]	$P2_1/c$	2.141(4)	1.13(5)	2.78	—	—	3.092(3)
2,6-xylyl$_3$SnH (**8**)	$P\bar{1}$	2.159(5)	—	2.87	2.70–2.81	—	—
mesityl$_2$SnH$_2$[28]	$C2/c$	2.154(9)	1.669(2)	—	2.70–2.75	—	—
phenyl$_3$SnBr[45]	$P2_1/c$	2.114(8)	2.495(2)	2.63–3.14	—	3.03	—
2,6-xylyl$_3$SnBr (**4**)	$P2_1/c$	2.164(8)	2.547(3)	—	2.78	3.03–3.10	—
mesityl$_3$SnBr[46]	$P\bar{1}$	2.169(5)	2.547(1)	3.17	3.01	2.96	—

Fig. 3. Crystal packing diagram for 2,6-xylyl$_3$SnBr (**4**). C–H···π interactions are highlighted by dashed bonds. All non-carbon atoms shown as 30% shaded ellipsoids. Hydrogen atoms not involved in intermolecular interactions removed for clarity.

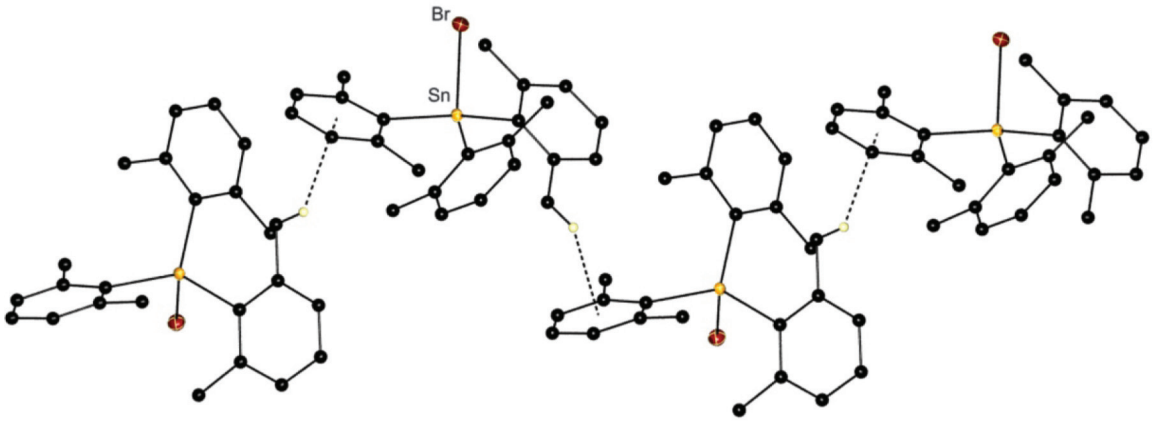

naphthyl substituents show a large propensity towards π–π stacking. In each case, molecules arrange to maximize these interactions, creating infinite layers of parallel stacked naphthalene derivatives with a specific distance between the ring centers (*d*). They are also found to be parallel-displaced to each other with a certain offset (*R*). This is in stark contrast to the previously mentioned herringbone structure present for naphthalene, which is dominated by edge to face interactions and corresponds more to larger polycyclic aromatic molecules, such as coronene, kekulene, or graphite.[29,52] 1-NaphthylSnCl$_3$ and 2-naphthylSnCl$_3$ (**6**) show similar interplanar distances of 3.56 and 3.54 respectively. These findings are in accordance with a reported range of 3.4–3.6 Å for benzene[29] or 3.35 Å in graphite.[52] 2-NaphthylSnCl$_3$ (**6**) shows a slightly larger displacement (*R*) of 1.76 Å. Offset distances for other benzyl systems are found in the range 1.6–1.8 Å.[29] In addition to π–π stacking, C–H···Cl interactions were observed between layers for both compounds (Table 4). If the number of naphthyl substituents is increased as seen in 1-naphthyl$_2$SnCl$_2$ (Fig. 6) and 2-naphthyl$_2$SnCl$_2$ (**6**), π–π stacking in the solid state is maintained, however, infinite linear chains are formed between neighbouring molecules.[2] 1-Naphthyl$_2$SnCl$_2$ shows an interplanar distance (*d*) of 3.60 Å, while 2-naphthyl$_2$SnCl$_2$ is packed slightly tighter with a distance of 3.40 Å.

Also exhibiting close π–π stacking interactions (d = 3.46, R = 1.65 Å) in the solid state is *o*-tolylSnCl$_3$ (**5**), which is a low temperature melting solid (4 °C), and subsequently obtaining a suitable solid state structure proved challenging (Table 4). Crystal packing diagrams of *o*-tolylSnCl$_3$ (**5**) display neighbouring molecules positioned to maximize C–H···π interactions from methyl groups (2.89 Å), while allowing π–π stacking interactions (Fig. 7). If methyl

Fig. 4. Crystal packing diagram for 2,6-xylyl$_3$SnH (**8**). Edge to face and C–H···π interactions are highlighted by dashed bonds. All non-carbon atoms shown as 30% shaded ellipsoids. Hydrogen atoms not involved in intermolecular interactions removed for clarity.

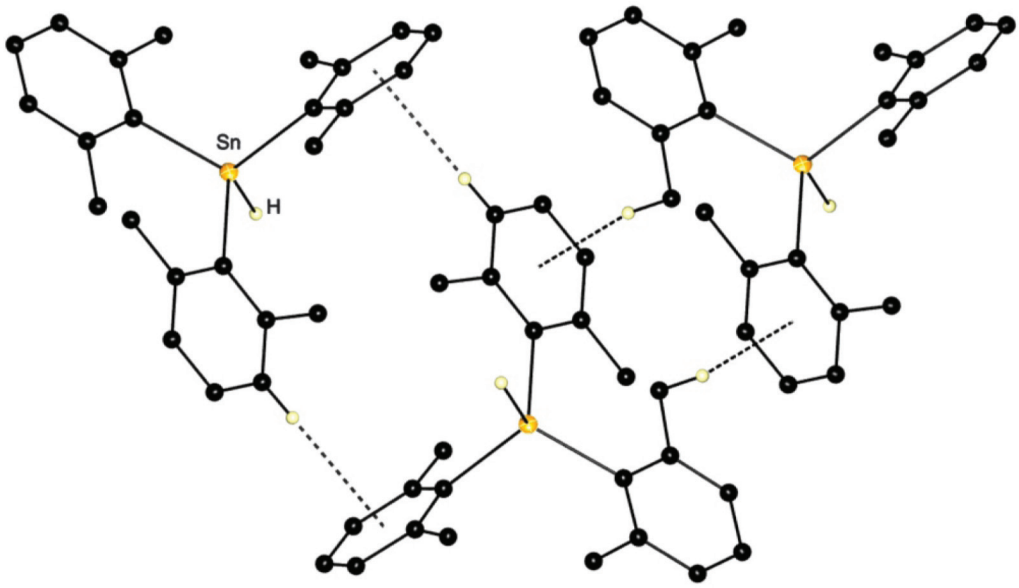

Table 4. List of Sn–C bond lengths and noncovalent interactions for aryltin tri- and dichlorides.

	Space group	Sn–C (Å) (avg)	Sn–Cl (Å) (avg)	Parallel displaced (Å)		Edge to face (Å)	C–H···π (Å)	C–H···Cl (Å)
				d	*R*			
o-tolylSnCl$_3$ (**5**)	*P*-1	2.109(4)	2.132(2)	3.46	1.65	—	2.89	2.95
2,6-xylylSnCl$_3$[2]	*Pbcn*	2.123(2)	2.332(1)	—	—	—	2.74	2.91
(2,6-Mes)PhSnCl$_3$[50]	$P2_1/c$	2.128(6)	2.332(1)	—	—	3.04	2.90	2.79
phenyl*SnCl$_3$[51]	*P*-1	2.155(5)	2.315(2)	—	—	—	3.15	—
1-naphthylSnCl$_3$[2]	$P2_1/c$	2.114(11)	2.324(3)	3.56	1.63	—	—	2.90
2-naphthylSnCl$_3$ (**6**)	*Pnma*	2.097(3)	2.306(7)	3.54	1.76	—	—	2.86
1-naphthyl$_2$SnCl$_2$[2]	*P*2/*n*	2.118(2)	2.359(1)	3.60	1.42	—	—	3.12
2-naphthyl$_2$SnCl$_2$[2]	$P2_1/n$	2.106(8)	2.354(19)	3.40	1.67	—	—	2.91

Note: Mes = (2,4,6-Me)Ph; phenyl* = (2,6-Trip)Ph, Trip = (2,4,6-iPr)Ph.

Fig. 5. Crystal packing diagram for 2-naphthylSnCl$_3$ (**6**). π–π stacking and C–H···Cl interactions are highlighted by dashed bonds. All non-carbon atoms shown as 30% shaded ellipsoids. Hydrogen atoms not involved in intermolecular interactions removed for clarity.

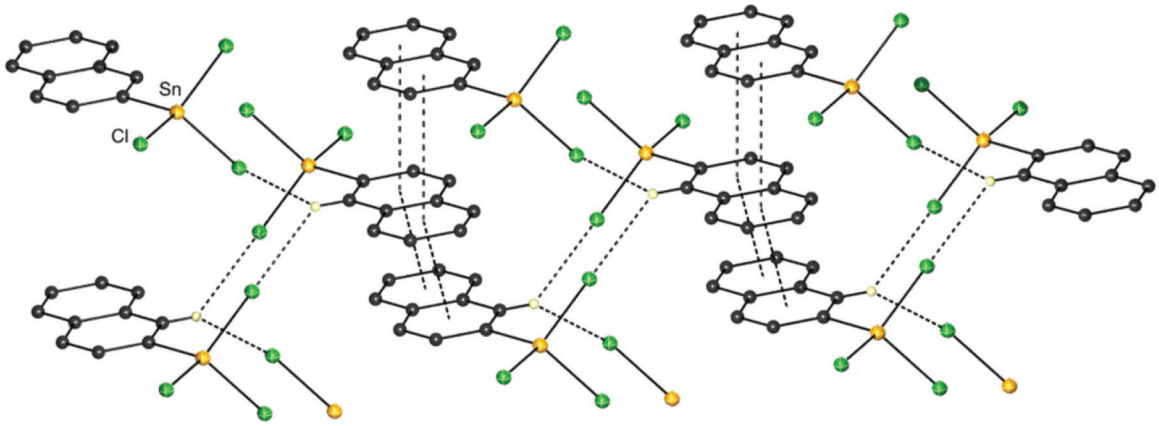

substitution is increased as seen for 2,6-xylylSnCl$_3$, only C–H···π interactions are present(2.74 Å).[2] It should be noted that *o*-tolylSnCl$_3$ displays the shortest Sn–Cl bond (2.132(2) Å) due to the lower steric hindrance afforded to the Sn atom by the *o*-tolyl substituent, compared to 2,6-xylylSnCl$_3$ (2.123(2) Å).

Conclusions

A series of novel organotin species containing methyl or *n*-butyl substituted phenyl and naphthyl residues have been synthesized and fully characterized by NMR spectroscopy and X-ray crystallography. In addition, the presence and nature of noncovalent inter-

Fig. 6. Crystal packing diagram for 1-naphthyl$_2$SnCl$_2$.[2] π–π stacking interactions are highlighted by dashed bonds. All non-carbon atoms shown as 30% shaded ellipsoids. Hydrogen atoms not involved in intermolecular interactions removed for clarity.

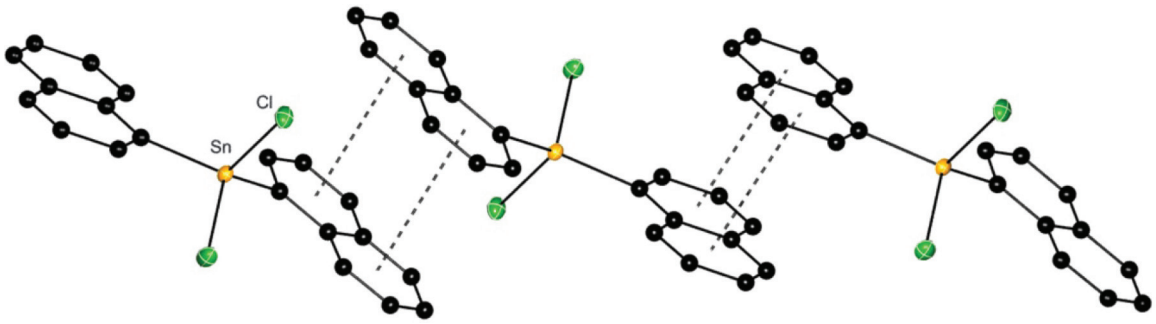

Fig. 7. Crystal packing diagram for *o*-tolylSnCl$_3$ (**5**). C–H···π and π–π stacking interactions are highlighted by dashed bonds. All non-carbon atoms shown as 30% shaded ellipsoids. Hydrogen atoms not involved in intermolecular interactions removed for clarity.

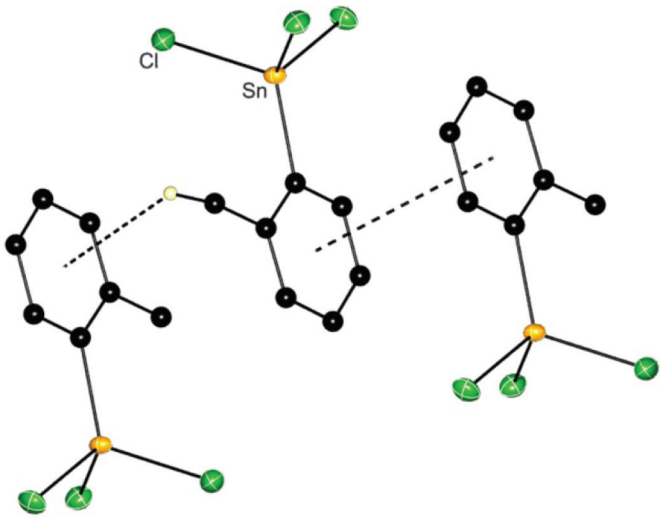

actions in the solid state of the presented compounds was studied and compared to those existing but never mentioned and simply overlooked in literature. Three different types of aromatic, non-covalent interactions could be detected, including the most prominent edge to face interaction, a parallel displaced π–π stacking as well as a C–H···π interaction of methyl groups to the neighbouring ring system. Edge to face interactions are found in the solid state structure of all presented organotins, mostly in the presence of additional interactions bringing about typical packing motifs. However, the discussed tetraarylstannanes 1-naphthyl$_4$Sn (**1**) and 2-naphthyl$_4$Sn (**2**) exclusively display edge to face interactions as stabilizing elements in the solid state. Substitution with aliphatic chains to the aromatic ring, as seen for *p*-*n*-butylphenyl$_4$Sn (**3**), results in both edge to face intermolecular and C–H···π interactions. 2-NaphthylSnCl$_3$ (**6**) and similar naphthyl tin mono- and dichlorides arrange themselves in the solid state to accommodate π–π stacking interactions through the naphthyl substituents of neighbouring molecules. Onefold and twofold methyl substitution in the ortho positions of the phenyl ring, in the case of *o*-tolylSnCl$_3$ (**5**) and 2,6-xylylSnCl$_3$, give rise to the coexistence of π–π stacking interactions through the aromatic rings as well as C–H···π interactions through the methyl groups and the aromatic rings of neighbouring substituents as stabilizing factors. Finally, the solid state structures of the novel tin monohydride 2,6-xylyl$_3$SnH (**8**) and monobromide 2,6-xylyl$_3$SnBr (**4**) presented, exhibit both edge to face intermolecular as well as C–H···π interactions.

Experimental

Materials and methods

All reactions, unless otherwise stated, were carried out using standard Schlenk line techniques under nitrogen atmosphere. All dried and deoxygenated solvents were obtained from a solvent drying system (Innovative Technology Inc). SnCl$_4$ anhydrous (98% *v*/*v*) was purchased at Alfa Aesar, distilled and stored under nitrogen. C$_6$D$_6$ was distilled over sodium and stored under nitrogen. All other chemicals from commercial sources (arylbromides and Ph$_3$SnCl) were utilized without further purification. All starting compounds, tetraaryl stannanes (Ar$_4$Sn) (**1–3**), were obtained according to published procedures; however, the work up procedure for *p*-butylphenyl$_4$Sn (**3**) was modified.[2,53] 2,6-Xylyl$_3$SnBr (**4**) was generated as the main product in the attempted synthesis of the corresponding tetraaryl stannane, as already mentioned in literature.[34] All aryltin trichlorides (**5–7**) were synthesized following the literature procedure via a Kozeshkov redistribution reaction.[35,37–38] Aryltin monohydride and trihydride were generated according to the preparation method of Finholt, Bond, and Schlesinger in Et$_2$O using lithium aluminum hydride (LiAlH$_4$) as reducing agent.[39] For already published compounds, only ^{1}H, ^{13}C, and ^{119}Sn NMR are provided. Elemental analysis was performed with an Elementar Vario EL III. Melting point measurements were carried out by three-fold determination with a Stuart Scientific SMP 10 (up to 300 °C).

NMR spectroscopy

^{1}H (300.22 MHz), ^{13}C (75.5 MHz), and ^{119}Sn (111.92 MHz) NMR spectra were recorded on a Mercury 300 MHz spectrometer from Varian at 25 °C. Chemical shifts are given in parts per million (ppm) relative to TMS (δ = 0 ppm) regarding ^{13}C and ^{1}H and relative to SnMe$_4$ in the case of ^{119}Sn. Coupling constants (*J*) are reported in Hertz (Hz). All NMRs were taken in C$_6$D$_6$. Reactions were monitored via ^{119}Sn NMR using a D$_2$O capillary as external lock signal. For complete peak assignment, multinuclear NMR experiments were also carried out (H,H-COSY and C,H-HETCOR) as well as shift comparisons to already known and similar compounds in literature were made.[2,54–55]

Crystal structure determination

All crystals suitable for single crystal X-ray diffractometry were removed from a Schlenk flask and immediately covered with a layer of silicone oil. Due to the low melting point of 4 °C for *o*-tolylSnCl$_3$ (**7**), the compound was recrystallized neat in the fridge and placed in silicon oil cooled down with dry ice. A single crystal was selected, mounted on a glass rod on a copper pin, and placed in the cold N$_2$ stream provided by an Oxford Cryosystems cryometer. XRD data collection was performed for compounds **1–6** and **8** on a Bruker Apex II diffractometer, with use of Mo Kα radiation (λ = 0.71073 Å) and a CCD area detector. Empirical absorption corrections were applied using SADABS.[56] The structures

Table 5. Crystallographic data and details of measurements for compounds **1–6** and **8**.

Compound	**1**	**2**	**3**	**4**	**5**	**6**	**8**
Formula	$C_{40}H_{28}Sn$	$C_{40}H_{28}Sn$	$C_{40}H_{52}Sn$	$C_{24}H_{27}BrSn$	$C_7H_7Cl_3Sn$	$C_{10}H_7Cl_3Sn$	$C_{24}H_{28}Sn$
Fw (g mol^{-1})	627.31	627.31	651.50	514.05	316.17	352.20	435.15
a (Å)	11.0020(3)	19.0493(17)	10.2809(3)	7.9774(3)	7.1993(8)	9.1965(3)	6.9415(4)
b (Å)	12.3126(4)	19.0493(17)	13.5926(4)	18.6305(6)	8.6524(10)	7.0776(2)	11.9714(7)
c (Å)	21.3522(6)	7.8388(8)	26.0182(8)	14.5078(4)	17.4519(19)	18.0394(5)	12.8316(8)
α (°)	90	90	92.532(2)	90	76.418(3)	90	108.672(2)
β (°)	90.789(1)	90	96.022(2)	94.680(1)	78.788(3)	90	91.291(2)
γ (°)	90	90	97.922(2)	90	81.902(4)	90	95.958(2)
V (Å^3)	2892.16(15)	2844.5(6)	3574.97(19)	2149.00(12)	1031.4(2)	1174.17(6)	1002.96(10)
Z	4	4	4	4	4	4	2
Crystal system	Monoclinic	Tetragonal	Triclinic	Monoclinic	Triclinic	Orthorhombic	Triclinic
Space group	$P2_1/n$	I-4	P-1	$P2_1/c$	P-1	$Pnma$	P-1
d_{calc} (Mg/m^3)	1.439	1.465	1.210	1.589	2.036	1.992	1.440
μ (mm^{-1})	0.91	0.93	0.74	3.05	3.19	2.82	1.28
T (K)	100(2)	100(2)	100(2)	100(2)	100(2)	100(2)	100(2)
2θ range (°)	2.5–25.9	2.8–27.6	2.3–26.5	2.6–26.8	2.4–27.2	2.5–27.1	2.8–26.4
F(000)	1272	1272	1368	1024	600	672	444
R_{int}	0.097	0.050	0.082	0.030	0.055	0.041	0.043
Independent reflns	5911	2833	15766	4448	4157	1397	4069
No. of params	358	185	767	241	201	82	236
R_1, $wR2$ (all data)[a]	R_1 = 0.1000	R_1 = 0.0429	R_1 = 0.0955	R_1 = 0.0250	R_1 = 0.0349	R_1 = 0.0232	R_1 = 0.0501
	$wR2$ = 0.1406	$wR2$ = 0.0940	$wR2$ = 0.1195	$wR2$ = 0.0474	$wR2$ = 0.0865	$wR2$ = 0.0540	$wR2$ = 0.1275
R_1, $wR2$ (>2σ)[b]	R_1 = 0.0597	R_1 = 0.0354	R_1 = 0.0535	R_1 = 0.0193	R_1 = 0.0347	R_1 = 0.0202	R_1 = 0.0480
	$wR2$ = 0.1246	$wR2$ = 0.0893	$wR2$ = 0.1076	$wR2$ = 0.0452	$wR2$ = 0.0864	$wR2$ = 0.0522	$wR2$ = 0.1260

Note: Mo Kα (λ = 0.71073 Å). $R_1 = \sum||F_o| - |F_c||/\sum|F_d|$; $wR_2 = [\sum_w(F_o^2 - F_2^2)^2/\sum_w(F_o^2)^2]^{1/2}$.

were solved using either direct methods or the Patterson option in SHELXS, and refined by the full-matrix least-squares procedures in SHELXL.[57–58] Non-hydrogen atoms were refined anisotropically. Hydrogen atoms were located in calculated positions corresponding to standard bond lengths and angles. For compound **1**, several restraints and constraints (FRAG 17, AFIX 173) were used to afford idealized naphthalene geometry for one of the naphthyl groups. Disorder was handled by modeling the occupancies of the individual orientations using free variables to refine the respective occupancy of the affected fragments. For compound **3**, disorder on one of the *n*-butyl groups was refined using 50/50 split positions. For compound **8**, the hydrogen atom bound to Sn was not found on the difference map and residual electron density is attributed to the heavy Sn atom. This is a common problem with locating light atoms (hydrogen) next to heavy atoms because of their poor scattering abilities. Intermolecular interactions for presented and published compounds based on a Cambridge Structural Database[59] search were determined by the calculation of centroids and planes feature of the programs Mercury[60] and Diamond.[61] Table 5 contains crystallographic data and details of measurements and refinement for compounds **1–6** and **8** (also, please see Supplementary data).

General procedure for Ar_4Sn and 2,6-xylyl$_3$SnBr (1–4)

A flask equipped with a dropping funnel and a reflux condenser was charged with Mg in THF. The dropping funnel was charged with arylbromide in THF. One mL of dibromoethane was added, and the solution was heated to start the reaction. The arylbromide was subsequently added slowly. After complete addition, the reaction was refluxed for 2 h. A second flask equipped with a mechanical stirrer and a reflux condenser was charged with $SnCl_4$ in THF cooled with an ice bath. The Grignard solution was then transferred via a cannula to the $SnCl_4$ solution whilst hot to avoid precipitation of the Grignard reagent. The solution was refluxed for 2 h and stirred overnight at RT. Three possible work-up procedures were carried out. In one case (**a**) the solution was filtered through celite and the solvent evaporated under reduced pressure. To the resulting residue, water was added and then extracted with dichloromethane. The organic phase was dried over Na_2SO_4, filtered, and the solvent evaporated under reduced pressure. The product was suspended in Et_2O, filtered, and washed with Et_2O and subsequently with pentane. The product was then dried in an oven at 110 °C overnight. Alternatively, (**b**) H_2O was added and subsequently all of the solvent was removed under reduced pressure. The resulting residue was taken up in pentane and refluxed until all of the product dissolved. The suspension was filtered again through celite and washed with pentane. The solvent was removed under reduced pressure, and the resulting oil was distilled under reduced pressure. Instead, (**c**) H_2O was added, and subsequently all of the solvent was removed under reduced pressure. The resulting residue was extracted with a soxhlet apparatus for 2 h with pentane. The pentane was evaporated under reduced pressure.

1-naphthyl$_4$Sn (1)

17.0 g (700 mmol, 7 equiv.) Mg in 700 mL THF, 83.4 mL (600 mmol, 6 equiv.) 1-bromonaphthalene in 150 mL THF, 11.7 mL (100 mmol, 1 equiv.) $SnCl_4$ in 1 L THF, work-up procedure (**a**): 1000 mL H_2O, 250 mL Et_2O, 250 mL Et_2O, 250 mL pentane. For analysis, a small amount was recrystallized from ethylacetate to obtain colorless crystals. Yield: 72% (45.2 g, 72.0 mmol). M.p.:, 230–232 °C. ^{1}H NMR (C_6D_6, 300 MHz): δ 8.33 (d, 4H, ^3J(H4-H3) = 8.3 Hz, H4), 8.12 (d, 4H, ^3J(H2-H3) = 6.6 Hz, H2), 7.62 (d, 4H, ^3J(H8-H7) = 8.2 Hz, H8), 7.54 (d, 4H, ^3J(H5-H6) = 8.1 Hz, H5), 7.12–7.00 (m, 8H, H6, H7), 6.83 (dd, 2H, H3) ppm. ^{13}C NMR (C_6D_6, 75.5 MHz): δ 140.7 (^1J(^{13}C-^{119}Sn) = 520 Hz, ^1J(^{13}C-^{117}Sn) = 497 Hz, C1), 139.4 (^2J(^{13}C-^{119}Sn) = 34.7 Hz, ^2J(^{13}C-^{117}Sn) = 33.8 Hz, C8a), 137.6 (^2J(^{13}C-$^{119/117}$Sn) = 38.1 Hz, C2), 134.5 (^3J(^{13}C-^{119}Sn) = 37.6 Hz, ^3J(^{13}C-^{117}Sn) = 36.4 Hz, C4a), 130.6 (^4J(^{13}C-$^{119/117}$Sn) = 32.2 Hz, C4), 130.3 (^3J(^{13}C-$^{119/117}$Sn) = 11.7 Hz, C8), 129.3 (^3J(^{13}C-$^{119/117}$Sn) = 43.8 Hz, C3), 126.4 (C7), 126.1 (C6) ppm. ^{119}Sn NMR (C_6D_6, 112 MHz): δ –118.8 ppm. Anal. calcd. for $C_{20}H_{14}Sn$: C, 76.58; H, 4.50. Found: C, 75.36; H, 4.40.

2-naphthyl$_4$Sn (2)

3.2 g (131 mmol, 4.5 equiv.) Mg in 250 mL THF, 25.9 g (125 mmol, 4.3 eq.) 2-bromonaphthalene in 50 mL THF, 3.4 mL (29.1 mmol, 1 equiv.) $SnCl_4$ in 500 mL of THF, work-up procedure (**a**): 250 mL l H_2O, 500 mL of dichloromethane, 100 mL Et_2O, 100 mL of Et_2O, 100 mL pentane. For analysis a small amount was recrystallized from ethylacetate to obtain colorless crystals. Yield: 56% (10.2 g,

16.2 mmol). M.p.: 199–200 °C. ^{1}H NMR (C_6D_6, 300 MHz): δ 8.14 (s, 4H, ^3J(H1-$^{119/117}$Sn) = 55.2 Hz, H1), 7.92 (d, 4H, ^3J(H3-H4) = 8.2 Hz, ^3J(H3-$^{119/117}$Sn) = 40.7 Hz, H3), 7.75 (d, 4H, ^3J(H4-H3) = 8.2 Hz, ^4J(H4-$^{119/117}$Sn) = 12.8 Hz, H4), 7.63 (d, 4H, ^3J(H8-H7) = 7.8 Hz, H8), 7.45 (d, 4H, ^3J(H5-H6) = 7.7 Hz, H5), 7.28–7.16 (m, 8H, H6, H7) ppm. ^{13}C NMR (C_6D_6, 75.5 MHz): δ 138.7 (^2J(^{13}C-^{119}Sn = 36.9 Hz, ^2J(^{13}C-^{117}Sn = 35.4 Hz, C1), (^1J(^{13}C-^{119}Sn = 529 Hz, ^1J(^{13}C-^{117}Sn = 505 Hz, C2), 134.5 (^4J(^{13}C-$^{119/117}$Sn = 9.9 Hz, C4a), 134.3 (^3J(^{13}C-^{119}Sn = 57.8 Hz, ^3J(^{13}C-^{117}Sn = 55.3 Hz, C8a), 133.7 (^2J(^{13}C-^{119}Sn = 40.3 Hz, ^2J(^{13}C-^{117}Sn = 38.7 Hz, C3), 128.6 (^3J(^{13}C-^{119}Sn = 50.6 Hz, ^3J(^{13}C-^{117}Sn = 48.3 Hz, C4), 128.3 (^5J(^{13}C-$^{119/117}$Sn = 4.6 Hz, C5), 128.2 (C8), 126.8 (C6), 126.4 (^5J(^{13}C-$^{119/117}$Sn = 4.3 Hz, C7) ppm. ^{119}Sn NMR (C_6D_6, 112 MHz): δ –117.6 ppm. Anal. calcd. for $C_{20}H_{14}$Sn: C, 76.58; H, 4.50. Found: C, 76.64; H, 4.46.

p-n-*butylphenyl$_4$Sn (3)*

14.3 g (0.59 mol, 5 equiv.) Mg in 270 mL THF, 100 g (0.47 mol, 4 equiv.) *p-n*-butylphenylbromide in 30 mL THF, 13.7 mL (0.12 mmol, 1 equiv.) $SnCl_4$ in 300 mL of THF, work-up procedure (**b**): 10 mL of H_2O to quench, refluxed in 800 mL of pentane, washed with 50 mL pentane. The resulting solid was recrystallized from *n*-BuOH in the fridge to obtain colorless crystals. Yield: 65% (53.9 g, 83 mmol). M.p.: 42 °C. ^{1}H NMR (C_6D_6, 300 MHz): δ 7.73 (d, 8H, ^3J(H2-H3) = 7.80 Hz, ^3J(^{1}H-^{119}Sn) = 48.1 Hz, ^3J(^{1}H-^{117}Sn) = 45.7 Hz, H2), 7.12 (d, 8H, ^3J(H3-H2) = 7.7 Hz, ^4J(^{1}H-$^{119/117}$Sn) = 13.9 Hz, H3), 2.52–2.40 (t, 8H, H5), 1.55–1.41 (dd, 8H, H6), 1.30–1.14 (dd, 8H, H7), 0.88–0.77 (t, 12H, H8) ppm. ^{13}C NMR (C_6D_6, 75.5 MHz): δ 143.9 (^4J(^{13}C-$^{119/117}$Sn) = 11.5 Hz, C4), 137.8 (^2J(^{13}C-^{119}Sn) = 39.2 Hz,^2J(^{13}C-^{117}Sn) = 36.9 Hz, C2), 135.4 (^1J(^{13}C-^{119}Sn) = 535 Hz,^1J(^{13}C-^{117}Sn) = 511 Hz, C1), 129.3 (^3J(^{13}C-^{119}Sn) = 53.0 Hz,^3J(^{13}C-^{117}Sn) = 50.7 Hz, C3), 36.0 (C5), 33.9 (C6), 22.6 (C7), 14.1 (C8) ppm. ^{119}Sn NMR (C_6D_6, 112 MHz): δ –121.5 ppm. Anal. calcd. for $C_{40}H_{52}$Sn: C, 73.74; H, 8.04. Found: C, 75.25; H, 8.04.

2,6-xylyl$_3$SnBr (4)

7.59 g (0.25 mol, 7.8 equiv.) Mg in 300 mL THF, 46.3 g (0.25 mol, 6.3 equiv.) 2,6-xylylbromide in 60 mL THF, 4.9 mL (0.04 mol, 1 equiv.) $SnCl_4$ in 100 mL of THF, work-up procedure (**c**) 1 L of pentane. The resulting solid was recrystallized from pentane to obtain colorless crystals. Yield: 90% (16.9 g, 36 mmol). M.p.: 175 °C. ^{1}H NMR (C_6D_6, 300 MHz): δ 7.03–6.96 (t, 3H, H4), 6.85 (d, 6H, ^3J(H3-H4) = 7.47 Hz,^4J(^{1}H-$^{119/117}$Sn) = 32.8 Hz, H3), 2.45 (s, 18H,^3J(^{1}H-$^{119/117}$Sn) = 6.50 Hz, CH_3) ppm. ^{13}C NMR (C_6D_6, 75.5 MHz): δ 145.0 (^1J(^{13}C-^{119}Sn) = 571 Hz,^1J(^{13}C-^{117}Sn) = 546 Hz, C1), 144.5 (^2J(^{13}C-^{119}Sn) = 43.9 Hz,^2J(^{13}C-^{117}Sn) = 42.0 Hz, C2), 130.1 (^3J(^{13}C-^{119}Sn) = 52.7 Hz,^3J(^{13}C-^{117}Sn) = 50.5 Hz, C3), 26.0 (^3J(^{13}C-^{119}Sn) = 41.8 Hz, ^3J(^{13}C-^{117}Sn) = 40.1 Hz, CH_3) ppm. ^{119}Sn NMR (C_6D_6, 112 MHz): δ –131.6 ppm. Anal. calcd. for $C_{24}H_{27}$BrSn: C, 56.07; H, 5.29. Found: C, 54.67; H, 5.48.

General procedure for $ArSnCl_3$ (5–7)

The corresponding tetraaryl stannane was combined with 3 equiv. of $SnCl_4$ in a Schlenk flask. The mixture was heated up to 150–160 °C using an oil bath and stirred for 1 h to obtain complete conversion. Residual $SnCl_4$ was removed under reduced pressure to obtain a dark brown residue. The mixture was subjected to fractionated distillation under reduced pressure to afford pure product in the case of liquid compounds (work-up procedure **a**). For solid products, the reaction mixture was suspended in dichloromethane, filtered through celite and the solvent evaporated under reduced pressure to afford solid compounds (work-up procedure **b**).

o-tolylSnCl$_3$(5)

13.4 g tetra-*o*-tolyltin (28 mmol, 1 equiv.), 9.7 mL $SnCl_4$ (21.6 g, 83 mmol, 3 equiv.), 150 °C, work-up procedure (**a**), Compound was crystallized neat at 4 °C. Yield: 95% (33.8 g, 106 mmol). M. p.: 9 °C. ^{1}H NMR (C_6D_6, 300 MHz): δ 7.21 (d, 1H,^3J(H6-H5) = 8.5 Hz,^4J(H6-$^{119/117}$Sn) = 64.6 Hz, H6), 7.06–6.97 (dd, 1H, H4), 6.91–6.82 (dd, 1H, H5), 6.81–6.76 (d, 1H, H3), 2.18 (s, 3H,^4J(H7-$^{119/117}$Sn) = 13.7 Hz, H6) ppm. ^{13}C NMR (C_6D_6, 75.5 MHz): δ 142.9 (^2J(^{13}C-^{119}Sn) = 75.2 Hz, ^2J(^{13}C-^{117}Sn) = 72.0 Hz, C2), 136.7 (^1J(^{13}C-^{119}Sn) = 1085 Hz, ^1J(^{13}C-^{117}Sn) = 1036 Hz, C1), 134.4 (^2J(^{13}C-^{119}Sn) = 77.8 Hz, ^2J(^{13}C-^{117}Sn) = 74.4 Hz, C6), 133.3 (^4J(^{13}C-$^{119/117}$Sn) = 23.9 Hz, C4), 131.6 (^3J(^{13}C-^{119}Sn) = 119 Hz, ^3J(^{13}C-^{117}Sn) = 114 Hz, C3), 127.2 (^3J(^{13}C-^{119}Sn) = 128 Hz, ^3J(^{13}C-^{117}Sn) = 122 Hz, C5), 24.3 (^3J(^{13}C-^{119}Sn) = 55.3 Hz, ^3J(^{13}C-^{117}Sn) = 53.4 Hz, C7) ppm. ^{119}Sn NMR (C_6D_6, 112 MHz): δ –60.7 ppm. Anal. calcd. for $C_7H_7Cl_3Sn$: C, 26.59; H, 2.23. Found: C, 26.12; H, 2.13.

2-naphthylSnCl$_3$ (6)

3.71 g tetra-2-naphthyltin **2** (5.7 mmol, 1 equiv.), 1.99 mL $SnCl_4$ (4.5 g, 17 mmol, 3 equiv.), 160 °C, work-up procedure (**b**) The resulting solid was recrystallized from chloroform to obtain colorless crystals. Yield: 90% (7.2 g, 20 mmol). M. p.: 82 °C. ^{1}H NMR (C_6D_6, 300 MHz): δ 7.64 (s, 1H, ^3J(H1-^{119}Sn) = 135.4 Hz, ^3J(H1-^{117}Sn) = 134.9 Hz, H1), 7.40–7.31 (m, 2H, H4, H6), 7.28–7.23 (m, 2H, H5, H7), 7.20–7.10 (m, 1H, H3), 7.04 (d, ^3J(H8-H7) = 8.38 Hz, H8).^{13}C NMR (C_6D_6, 75.5 MHz): δ 136.0 (^2J(^{13}C-^{119}Sn) = 74.6 Hz, ^2J(^{13}C-^{117}Sn) = 71.5 Hz, C1), 135.1 (^4J(^{13}C-$^{119/117}$Sn) = 23.1 Hz, C4a), 133.4 (^3J(^{13}C-^{119}Sn) = 141.4 Hz, ^3J(^{13}C-^{117}Sn) = 135.3 Hz, C8a), 135.2 (^1J(^{13}C-^{119}Sn) = 1130 Hz, ^1J(^{13}C-^{117}Sn) = 1081 Hz, C2), 130.1 (^3J(^{13}C-^{119}Sn) = 124.7 Hz, ^3J(^{13}C-^{117}Sn) = 119.3 Hz, C4), 128.8 (^5J(^{13}C-$^{119/117}$Sn = 5.5, C5/C7), 128.7 (^5J(^{13}C-$^{119/117}$Sn = 5.8 Hz, C5/C7), 128.2 (C6), 128.1 (^2J(^{13}C-^{119}Sn) = 85.4 Hz, ^2J(^{13}C-^{117}Sn) = 81.8 Hz, C3), 127.4 (^4J(^{13}C-$^{119/117}$Sn = 11.3 Hz, C8).^{119}Sn NMR (C_6D_6, 112 MHz): δ –63.5 ppm. Anal. calcd. for $C_{10}H_7Cl_3Sn$: C, 34.10; H, 2.00. Found: C, 35.82; H, 2.13.

p-n-*butylphenylSnCl$_3$ (7)*

2.0 g tetra-*p-n*-butyltin **3** (3.1 mmol, 1 equiv.), 1.07 mL $SnCl_4$ (2.4 g, 9.2 mmol, 3 equiv.), 150 °C, work-up procedure (**a**) Yield: 87% ^{1}H NMR (C_6D_6, 300 MHz): δ 6.99 (d, 2H, ^3J(H3-H2) = 7.9 Hz, H3), 6.75 (d, 2H, ^3J(H2-H3) = 7.8 Hz, ^3J(H2-$^{119/117}$Sn) = 48.5 Hz, H2), 2.21 (t, 2H, H5), 1.37–1.21 (dd, 2H, H6), 1.20–1.04 (dd, 2H, H7), 0.81 (t, 3H, H8) ppm. ^{13}C NMR (C_6D_6, 75.5 MHz): δ 148.6 (^4J(^{13}C-^{119}Sn) = 28.8 Hz, ^4J(^{13}C-^{117}Sn) = 25.4 Hz, C4), 133.9 (^2J(^{13}C-^{119}Sn) = 82.2 Hz, ^2J(^{13}C-^{117}Sn) = 80.0 Hz, C2), 133.9 (^1J(^{13}C-^{119}Sn) = 1137 Hz, ^1J(^{13}C-^{117}Sn) = 1083 Hz, C1), 130.5 (^3J(^{13}C-^{119}Sn) = 130.2 Hz, ^3J(^{13}C-^{117}Sn) = 124.8 Hz, C3), 35.7 (^5J(^{13}C-$^{119/117}$Sn) = 12.4 Hz, C5), 33.4 (^6J(^{13}C-$^{119/117}$Sn = 5.8 Hz, C6), 22.5 (C7), 14.0 (C8) ppm. ^{119}Sn NMR (C_6D_6, 112 MHz): δ –58.2 ppm.

General procedure for Ar_3SnH and $ArSnH_3$

A flask furnished with a reflux condenser and a dropping funnel was charged $LiAlH_4$ pellets and Et_2O. A solution of arytltin trichloride in Et_2O was added slowly via the dropping funnel while cooling to either 0 °C or –30 °C. The reaction mixture was stirred for 1 h and allowed to warm up to RT. Subsequently, degassed water was added. The phases were separated via a cannula, and the aqueous layer washed twice with Et_2O. The combined organic phases were extracted with saturated sodium tartrate in degassed water, and the resulting organic phase dried over $CaCl_2$. For 2,6-xylyl$_3$SnH (**8**), the solvent was evaporated under reduced pressure to afford a solid product. For *p-n*-butylphenylSnH_3 (**9**), the solvent was evaporated gently at 200 mbar (1 bar = 100 kPa), and the product was distilled at RT using the turbomolecular pump, while the receiving flask was placed in a dewar filled with liquid nitrogen to obtain a colorless liquid.

2,6-xylyl$_3$SnH (8)

5.38 g tri-2,6-xylyltinbromide **4** (10.5 mmol, 1 equiv.) in 40 mL Et_2O, 0.60 g LAH pellets (15.7 mmol, 1.5 equiv.) in 40 mL Et_2O, 50 mL degassed H_2O, 2 × 40 mL Et_2O. The resulting solid was recrystallized from toluene to obtain colorless crystals. Yield: 57% (2.59 g, 59.5 mmol). M.p.: 139 °C. ^{1}H NMR (C_6D_6, 300 MHz): δ 7.09–7.02 (t, 3H, H4), 6.91 (d, 6H, ^3J(H3-H4) = 7.6, H3), 6.86 (s, 1H, ^1J(^{1}H-^{119}Sn) = 1776 Hz, ^1J(^{1}H-^{117}Sn) = 1697 Hz, Sn-H), 2.32 (s, 6H, CH_3) ppm. ^{13}C NMR (C_6D_6, 75.5 MHz): δ 145.0 (^2J(^{13}C-$^{119/117}$Sn) = 32.5 Hz, C2), 142.9 (^1J(^{13}C-^{119}Sn) = 534 Hz,^1J(^{13}C-^{117}Sn) = 511 Hz, C1), 129.3 (^4J(^{13}C-

$^{119/117}$Sn) = 9.4 Hz, C4), 127.7 (^{3}J(^{13}C-^{119}Sn) = 43.8 Hz,^{3}J(^{13}C-^{117}Sn) = 41.5 Hz, C3), 25.8 (^{3}J(^{13}C-^{119}Sn) = 42.6 Hz,^{3}J(^{13}C-^{117}Sn) = 40.3 Hz, *C*H$_3$) ppm.^{119}Sn NMR (C_6D_6, 112 MHz): δ –286.6 (^{1}J($^{119/117}$Sn-^{1}H) = 1780 Hz) ppm. Anal. calcd. for $C_{10}H_7Cl_3Sn$: C, 66.24; H, 6.49. Found: C, 67.94; H, 6.78.

p-n-*butylphenylSnH$_3$ (9)*

5.0 g *p*-butylphenylSnCl$_3$ **7** (14.0 mmol, 1 equiv.) in 40 mL Et$_2$O 1.1 g LiAlH$_4$ pellets (27.9 mmol, 2 equiv.) in 40 mL Et$_2$O, 50 mL degassed H$_2$O, 2 × 40 mL Et$_2$O. Yield: 83% (2.95 g, 11.5 mmol). ^{1}H NMR (C_6D_6, 300 MHz): 7.30 (d, 2H, ^{3}J(H2-H3) = 6.96, ^{3}J(H2-$^{119/117}$Sn) = 55.9 Hz, H2), 6.99 (d, 2H, ^{3}J(H3-H2) = 7.0 Hz, ^{3}J(H3-$^{119/117}$Sn) = 24.8 Hz, H3), 5.05 (s, 3H, ^{1}J(^{1}H-^{119}Sn = 1913 Hz, ^{1}J(^{1}H-^{117}Sn = 1828 Hz, Sn-H), 2.47–2.37 (t, 2H, H5), 1.52–1.39 (dd, 2H, H6), 1.30–1.15 (dd, 2H, H7), 0.09–0.80 (t, 3H, H8). ^{13}C NMR (C_6D_6, 75.5 MHz): 143.8 (^{4}J(^{13}C-$^{119/117}$Sn = 11.9 Hz, C4), 138.1 (^{2}J(^{13}C-^{119}Sn) = 45.2 Hz, ^{2}J(^{13}C-^{117}Sn) = 42.7 Hz, C2), 129.1 (^{3}J(^{13}C-^{119}Sn) = 62.6 Hz, ^{3}J(^{13}C-^{117}Sn) = 56.3 Hz, C3), 129.0 (^{1}J(^{13}C-^{119}Sn) = 571.2 Hz, ^{1}J(^{13}C-^{117}Sn) = 545.5 Hz, C1), 35.9 (C5), 33.9 (C6), 22.6 (C7), 14.1 (C8) ppm.^{119}Sn NMR (C_6D_6, 112 MHz): δ –344.6 ppm (^{1}J($^{119/117}$Sn-^{1}H) = 1910 Hz) ppm. Anal. calcd. for $C_{10}H_{16}Sn$: C, 47.11; H, 6.40. Found: C, 47.88.; H, 6.38.

Supplementary data

Supplementary data are available with the article through the journal Web site at http://nrcresearchpress.com/doi/suppl/10.1139/cjc-2013-0503. CCDC 969150-969156 contain the supplementary crystallographic data for compounds **1–6** and **8** respectively. These data can be obtained, free of charge, via http://www.ccdc.cam.ac.uk/products/csd/request (Or from the Cambridge Crystallographic Data Centre, 12 Union Road, Cambridge CB2 1E2, UK; fax: +44 1223 33603; or e-mail: deposit@ccdc.cam.ac.uk).

Acknowledgements

This work was supported by the NAWI Graz project, a collaboration between the Graz University of Technology and the Graz University and the COST Action 1302 “Smart Inorganic Polymers”.

References

(1) Schneider-Koglin, C.; Mathiasch, B.; Dräger, M. *J. Organomet. Chem.* **1994**, *469* (1), 25. doi:10.1016/0022-328X(94)80074-X.
(2) Zeppek, C.; Pichler, J.; Torvisco, A.; Flock, M.; Uhlig, F. *J. Organomet. Chem.* **2013**, *740*, 41. doi:10.1016/j.jorganchem.2013.03.012.
(3) Chieh, P. C.; Trotter, J. *J. Chem. Soc. A* **1970**, 911. doi:10.1039/j19700000911.
(4) Belskii, V. K.; Simonenko, A. A.; Reikhsfeld, V. O.; Saratov, I. E. *J. Organomet. Chem.* **1983**, *244*, 125. doi:10.1016/S0022-328X(00)98592-9.
(5) Karipides, A.; Oertel, M. *Acta Crystallogr., Sect. B: Struct. Crystallogr. Cryst. Chem.* **1977**, *33* (3), 683. doi:10.1107/S0567740877004464.
(6) Karipides, A.; Wolfe, K. *Acta Crystallogr., Sect. B: Struct. Crystallogr. Cryst. Chem.* **1975**, *31* (2), 605. doi:10.1107/S0567740875003366.
(7) Wharf, I.; Belanger-Gariepy, F. *Acta Crystallogr., Sect. E: Struct. Rep. Online* **2003**, *59* (8), 661. doi:10.1107/S1600536803016167.
(8) Shaikh, N. S.; Parkin, S.; Lehmler, H.-J. *Organometallics* **2006**, *25* (17), 4207. doi:10.1021/om060456a.
(9) Wharf, I.; Lebuis, A.-M. *Main Group Met. Chem.* **2000**, *23*, 497. doi:10.1515/mgmc.2000.23.9.497.
(10) Bokii, N. G.; Zakharova, G. N.; Struchkov, Y. T., *J. Struct. Chem.* **1970**, 11 (5), 828. doi:10.1007/bf00743390.
(11) Geller, J. M.; Butler, I. S.; Gilson, D. F. R.; Morin, F. G.; Wharf, I.; Bélanger-Gariépy, F. *Can. J. Chem.* **2003**, *81* (11), 1187. doi:10.1139/v03-115.
(12) Wharf, I.; Simard, M. G.; McGinn, K. *Acta Crystallogr., Sect. C: Cryst. Struct. Commun.* **1995**, *51* (2), 236. doi:10.1107/S010827019400987X.
(13) Geller, J.; Wharf, I.; Belanger-Gariepy, F.; Lebuis, A.-M.; Butler, I. S.; Gilson, D. F. R. *Acta Crystallogr., Sect. C: Cryst. Struct. Commun.* **2002**, *58* (9), m466. doi:10.1107/S0108270102012362.
(14) Wharf, I.; Simard, M. G. *Acta Crystallogr., Sect. C: Cryst. Struct. Commun.* **1991**, *47* (8), 1605. doi:10.1107/S0108270191000537.
(15) Wharf, I.; Simard, M. G. *J. Organomet. Chem.* **1997**, *532* (1–2), 1. doi:10.1016/S0022-328X(96)06782-4.
(16) Wharf, I.; Lebuis, A.-M.; Roper, G. A. *Inorg. Chim. Acta* **1999**, *294* (2), 224. doi:10.1016/S0020-1693(99)00342-4.
(17) Wharf, I.; Lebuis, A.-M. *Acta Crystallogr., Sect. C: Cryst. Struct. Commun.* **1996**, *52* (12), 3025. doi:10.1107/S0108270196012115.
(18) Coffer, P. K.; Dillon, K. B.; Howard, J. A. K.; Yufit, D. S.; Zorina, N. V. *Dalton Trans.* **2012**, *41* (15), 4460. doi:10.1039/c2dt12369j.
(19) Bojan, R. V.; López-de-Luzuriaga, J. M.; Monge, M.; Olmos, M. E. *J. Organomet. Chem.* **2010**, *695* (22), 2385. doi:10.1016/j.jorganchem.2010.07.019.
(20) Sharma, H. K.; Cervantes-Lee, F.; Mahmoud, J. S.; Pannell, K. H. *Organometallics* **1999**, *18* (3), 399. doi:10.1021/om9805234.
(21) Baxter, J. L.; Holt, E. M.; Zuckerman, J. J. *Organometallics* **1985**, *4* (2), 255. doi:10.1021/om00121a009.
(22) Greene, P. T.; Bryan, R. F. *J. Chem. Soc. A* **1971**, 2549. doi:10.1039/J19710002549.
(23) Leonhardt, T.; Latscha, H. P. *Z. Naturforsch., B: Chem. Sci.* **1997**, *52*, 25.
(24) Kräuter, T.; Neumüller, B. *Z. Naturforsch., B: Chem. Sci.* **1998**, *53*, 503.
(25) Miles, D.; Burrow, T.; Lough, A.; Foucher, D. *J. Inorg. Organomet. Polym. Mater.* **2010**, *20* (3), 544. doi:10.1007/s10904-010-9376-3.
(26) Batsanov, A. S.; Cornet, S. M.; Dillon, K. B.; Goeta, A. E.; Thompson, A. L.; Yu Xue, B. *Dalton Trans.* **2003**, (12), 2496. doi:10.1039/b302544f.
(27) Weidenbruch, M.; Schäfers, K.; Pohl, S.; Saak, W.; Peters, K.; von Schnering, H. G. *J. Organomet. Chem.* **1988**, *346* (2), 171. doi:10.1016/0022-328X(88)80113-X.
(28) Schittelkopf, K.; Fischer, R. C.; Meyer, S.; Wilfling, P.; Uhlig, F. *Appl. Organomet. Chem.* **2010**, *24* (12), 897. doi:10.1002/aoc.1740.
(29) Meyer, E. A.; Castellano, R. K.; Diederich, F. *Angew. Chem., Int. Ed.* **2003**, *42* (11), 1210. doi:10.1002/anie.200390319.
(30) Jennings, W. B.; Farrell, B. M.; Malone, J. F. *Acc. Chem. Res.* **2001**, *34* (11), 885. doi:10.1021/ar0100475.
(31) Janiak, C. *J. Chem. Soc., Dalton Trans.* **2000**, 3885. doi:10.1039/b003010o.
(32) Hunter, C. A.; Sanders, J. K. M. *J. Am. Chem. Soc.* **1990**, *112* (14), 5525. doi:10.1021/ja00170a016.
(33) Nayak, S. K.; Sathishkumar, R.; Row, T. N. G. *CrystEngComm* **2010**, *12* (10), 3112. doi:10.1039/c001190h.
(34) Brown, P.; Mahon, M. F.; Molloy, K. C. *J. Organomet. Chem.* **1992**, *435* (3), 265. doi:10.1016/0022-328X(92)83397-Z.
(35) Kozeshkov, K. A. *Ber. Dtsch. Chem. Ges. B* **1929**, *62B*, 996. doi:10.1002/cber.19290620438.
(36) Buckton, G. B. *Justus Liebigs Ann. Chem.* **1859**, *112* (2), 220. doi:10.1002/jlac.18591120214.
(37) Kozeshkov, K. A. *Ber. Dtsch. Chem. Ges. B* **1933**, *66* (11), 1661. doi:10.1002/cber.19330661109.
(38) Kozeshkov, K. A.; Nadj, M. M. *Ber. Dtsch. Chem. Ges. B* **1934**, *5*, 717. doi:10.1002/cber.19340670502.
(39) Finholt, A. E.; Bond, A. C.; Wilzbach, K. E.; Schlesinger, H. I. *J. Am. Chem. Soc.* **1947**, *69* (11), 2692. doi:10.1021/ja01203a041.
(40) Dillard, C. R.; McNeill, E. H.; Simmons, D. E.; Yeldell, J. B. *J. Am. Chem. Soc.* **1958**, *80* (14), 3607. doi:10.1021/ja01547a031.
(41) Ingham, R. K.; Rosenberg, S. D.; Gilman, H. *Chem. Rev.* **1960**, *60* (5), 459. doi:10.1021/cr60207a002.
(42) Wharf, I. *Inorg. Chim. Acta* **1989**, *159* (1), 41. doi:10.1016/S0020-1693(00)80893-2.
(43) Brock, C. P.; Dunitz, J. D. *Acta Crystallogr., Sect. B: Struct. Crystallogr. Cryst. Chem.* **1982**, *38* (8), 2218. doi:10.1107/S0567740882008358.
(44) Pichler, J.; Torvisco, A.; Uhlig, F. *Can. J. Chem.* **2013**, doi:10.1139/cjc-2013-0504.
(45) Preut, H.; Huber, F. *Acta Crystallogr., Sect. B: Struct. Crystallogr. Cryst. Chem.* **1979**, *B35*, 744. doi:10.1107/s0567740879004635.
(46) Dakternieks, D.; Lim, A. E. K.; Tiekink, E. R. T. *Main Group Met. Chem.* **2000**, *23*, 325. doi:10.1515/mgmc.2000.23.5.325.
(47) Zard, S. Z. *Radical Reactions in Organic Synthesis*; Oxford University Press, 2003.
(48) Choffat, F.; Smith, P.; Caseri, W. *J. Mater. Chem.* **2005**, *15* (18), 1789. doi:10.1039/b417401c.
(49) Bukalov, S. S.; Leites, L. A.; Lu, V.; Tilley, T. D. *Macromolecules* **2002**, *35*, 1757. doi:10.1021/ma011249j.
(50) Ahmad, S. U.; Beckmann, J.; Duthie, A. *Chem. Asian J.* **2010**, *5* (1), 160. doi:10.1002/asia.200900436.
(51) Johnson, B. P.; Almstätter, S.; Dielmann, F.; Bodensteiner, M.; Scheer, M. *Z. Anorg. Allg. Chem.* **2010**, *636* (7), 1275. doi:10.1002/zaac.201000029.
(52) Bernal, J. D. *Proc. R. Soc. Lond. A* **1924**, *106* (740), 749. doi:10.1098/rspa.1924.0101.
(53) Schneider-Koglin, C.; Behrends, K.; Dräger, M. *J. Organomet. Chem.* **1993**, *448* (1–2), 29. doi:10.1016/0022-328X(93)80063-H.
(54) Bullpitt, M.; Kitching, W.; Adcock, W.; Doddrell, D. *J. Organomet. Chem.* **1976**, *116* (2), 161. doi:10.1016/S0022-328X(00)91791-1.
(55) Schaeffer, C. D.; Lefferts, J. L.; Zuckerman, J. J. *Org. Magn. Reson.* **1984**, *22* (2), 125. doi:10.1002/mrc.1270220215.
(56) Blessing, R. *Acta Crystallogr., Sect. A: Found. Crystallogr.* **1995**, *51* (1), 33. doi:10.1107/S0108767394005726.
(57) Sheldrick, G. *Acta Crystallogr., Sect. A: Found. Crystallogr.* **1990**, *46* (6), 467. doi:10.1107/S0108767390000277.
(58) Sheldrick, G. *Acta Crystallogr., Sect. A: Found. Crystallogr.* **2008**, *64* (1), 112. doi:10.1107/S0108767307043930.
(59) Allen, F. H. *Acta Crystallogr., Sect. B: Struct. Sci.* **2002**, *B58*, 380. doi:10.1107/s0108768102003890.
(60) Macrae, C. F.; Bruno, I. J.; Chisholm, J. A.; Edgington, P. R.; McCabe, P.; Pidcock, E.; Rodriguez-Monge, L.; Taylor, R.; van de Streek, J.; Wood, P. A. *J. Appl. Crystallogr.* **2008**, *41* (2), 466. doi:10.1107/S0021889807067908.
(61) Putz, H.; Brandenburg, K. *Diamond - Crystal and Molecular Structure Visualization*; 3.2i; **2012**, Crystal Impact: Bonn, Germany.